Data-Driven Based Eco-Driving Control for Plug-in Hybrid Electric Vehicles

Jie Li[1], Yonggang Liu[1*], Yuanjian Zhang[2], Zhenzhen Lei[3], Zheng Chen[4,5*] and Guang Li[5]

[1]State Key Laboratory of Mechanical Transmissions & School of Automotive Engineering, Chongqing University 400044, Chongqing, China
[2]School of Mechanical and Aerospace Engineering, Queen's University of Belfast, BT9 5AG, Northern Ireland
[3]School of Mechanical and Power Engineering, Chongqing University of Science & Technology 401331, Chongqing China
[4]Faculty of Transportation Engineering, Kunming University of Science and Technology 650500, Kunming, China
[5]School of Engineering and Materials Science, Queen Mary University of London, London, E1 4NS, United Kingdom
lijiecqu2015@163.com, andylyg@umich.edu, y.zhang@qub.ac.uk, 2010048@cqust.edu.cn, chen@kust.edu.cn, g.li@qmul.ac.uk
Correspondence: Yonggang Liu (andylyg@umich.edu), Zheng Chen (chen@kust.edu.cn)

Abstract: With the development of connected and automated vehicles, eco-driving control is reckoned to generate unprecedented potential on energy-saving in electrified powertrain. In this paper, a data-driven based eco-driving control strategy with efficient computation capacity is proposed for plug-in hybrid electric vehicles to achieve approximate optimal energy economy. An efficient hierarchical optimal control scheme is designed to mitigate the massive computational cost during velocity optimization and powertrain control. A data-driven optimal energy consumption cost model and an optimal battery current model are respectively constructed via two neural networks and served as the critic model and the system model during velocity optimization. Furthermore, the neural network-based dynamic programming is exploited to optimize the vehicle velocity by merging the data-driven models and Bellman optimality principle. The simulation results demonstrate that the proposed method can remarkably improve fuel economy by up to 16.7% in complicated driving conditions, compared with conventional sequential optimization methods. Furthermore, the data-driven control scheme can drastically improve the computational efficiency with slight sacrifice on fuel economy, compared with the optimum benchmark.

Key Words: Eco-driving, neural network, energy management, data-driven, plug-in hybrid electric vehicle

I. INTRODUCTION

Vehicle electrification supplies an efficient path to reduce the dependence on fossil fuel energy, and electric vehicles (EVs) and hybrid EVs (HEV) dominate the development trend among all feasible solutions [1, 2]. Moreover,

plug-in HEVs (PHEVs) are also widely adopted due to the operation mode incorporation of EVs and HEVs, which, in turn, complicates the design of control algorithms, including energy allocation scheme among different energy sources (usually internal combustion engine (ICE) and lithium-ion battery pack). On this account, the so-called energy management strategies (EMSs) are intensively investigated to allocate energy distribution and promote energy controlling performance of PHEVs, with the target of fuel economy optimization, battery lifespan extension, and driving experience promotion [3-5]. On the other hand, the flourishment of connected and automated technologies allows vehicles to easily access surrounding driving conditions, and thus brings in opportunities for velocity planning and subsequent energy saving, referred to as eco-driving [6-8]. In view of these optimization aspects, the combination of eco-driving optimization and simultaneous proper energy management may provide an unprecedented perspective to further improve the fuel economy of PHEVs. In this context, the conventional eco-driving has been gradually augmented to the extended eco-driving involving speed planning and energy allocation optimization.

The target of traditional eco-driving control problems is to optimize speed profiles of vehicle for fuel economy promotion. The initial attempt of eco-driving research concentrates on reference driving speed planning for drivers to avoid unnecessary acceleration and deceleration, so as to reduce fuel consumption [9]. While, the development of connected and automated technologies broadens the possibility of velocity planning for PHEVs according to the perceived surrounding and pre-known future driving conditions [10]. Currently, pulse and glide strategies are recognized as a widely accepted eco-driving scheme for intelligent ICE driven vehicle [11, 12], and they usually consist of rapid acceleration and coasting deceleration operations for optimizing the working range of ICE. In addition, optimization algorithms have been applied to achieve eco-driving, such as dynamic programming (DP) [13], pseudo-spectral method [14], and Pontryagin's Minimal Principle (PMP) [15]. For EVs, an analytical state-constrained control is implemented for eco-driving control in [16]. In [17], the global optimal eco-driving problem of EVs is solved through sequential quadratic programming. Additionally, some researches pay attention to optimize the velocity profiles according to the state of traffic lights [18]. In [19], a cooperative eco-driving system is designed to reduce the overall fuel consumption of traffic network at signalized intersections, where DP is exploited for optimal velocity planning and eco-driving control based on the queue prediction [20].

Moreover, hybridization in powertrain of PHEVs raises new challenges to eco-driving control [21]. The

powertrain system of PHEVs is more complex, and insufficient consideration of power distribution characteristics can affect the designated speed/acceleration to a large extent. Consequently, to reach the optimization of velocity profiles, EMS needs to be integrated into eco-driving control. However, the increase of state and control variables complicates the optimization design and augments the computation intensity. As such, sequential optimization is widely leveraged to solve the simultaneous optimization problem in a step-by-step manner, and decomposes the optimization of speed planning and energy management into two subsequent procedures [22, 23]. The mechanism of sequential optimization is shown in Fig. 1 (a). In the first step, the velocity profile is optimized to reduce energy consumption, and for the vehicle driven by ICE, the fuel consumption is typically defined as the cost function [24]. Whereas for PHEV, the fuel consumption cannot be directly calculated according to the driving state (including driving speed, acceleration and SOC), due to the existence of two power sources in powertrain. Thus, the net energy consumed by the motion of PHEV is usually defined as the objective function [25]. In the second step, the energy management is optimized according to the velocity profiles generated in the first step. The energy consumption cost of powertrain can be defined as the objective function in the second step. In [26], PMP is exploited to sequentially optimize the speed and energy management for HEV with the consideration of road grade. Ref. [27] investigates the effect of hierarchical eco-driving control in car-following scenarios based on model predictive control (MPC) and DP. In [28], a bi-level eco-driving control strategy based on MPC is proposed for connected and automated HEVs, and verified effective in reducing fuel consumption under complex driving conditions, including free driving, signal waiting and car-following scenarios. In addition, the energy management solutions in lower level controller can also supply the reversed guideline to the upper level controller, contributing to velocity planning [29]. Despite the preferable performance of sequential optimization, it is still troublesome to explicitly decouple the interaction between velocity planning and energy management of PHEVs, and the velocity trajectory planned previously may not be qualified to reach the optimal fuel economy of vehicle powertrain. That is, the EMS may only raise the minimum energy consumption under the suboptimal velocity planning; as such, the global optimal fuel economy in the whole trip cannot be guaranteed.

To further improve the overall fuel economy of PHEVs, a slew of efforts have been made on attaining co-optimization based eco-driving control [30, 31]. The co-optimization scheme, as shown in Fig. 1 (b), is an intuitive approach to overcome the insufficient decoupling existing in sequential optimization methods. The main difference

between co-optimization and sequential optimization methods lies in optimization procedure and optimization performance. Compared with sequential optimization methods, co-optimization methods typically optimize the velocity and energy management integrally to realize the efficient coupling between velocity and energy management, and the vehicle motion model and powertrain model are inputted for the velocity and energy management optimization to minimize the powertrain energy consumption. From this point of view, the velocity planning results can also be the solutions to the optimal powertrain energy consumption. Ref. [25] designs a PMP based strategy to simultaneously conduct velocity planning and energy allocation for a series HEV. In [32], a co-optimization based eco-driving control for fuel cell hybrid vehicle is proposed by applying DP and PMP, and a remarkable hydrogen economy improvement is attained. However, to the authors' knowledge, conventional co-optimization methods are not pragmatic for implementation because of their intensive computational burden, and the existence of multiple state and control variables increases the difficulty of solving the problem exponentially. Since sequential optimization is difficult to achieve the optimal fuel economy due to the incapacity in decoupling velocity planning and energy management, and co-optimization methods are limited by intensive calculation, designing a computationally efficient eco-driving method deserves to be investigated to further improve the fuel economy of PHEVs while incorporating the advantages of sequential optimization and co-optimization methods.

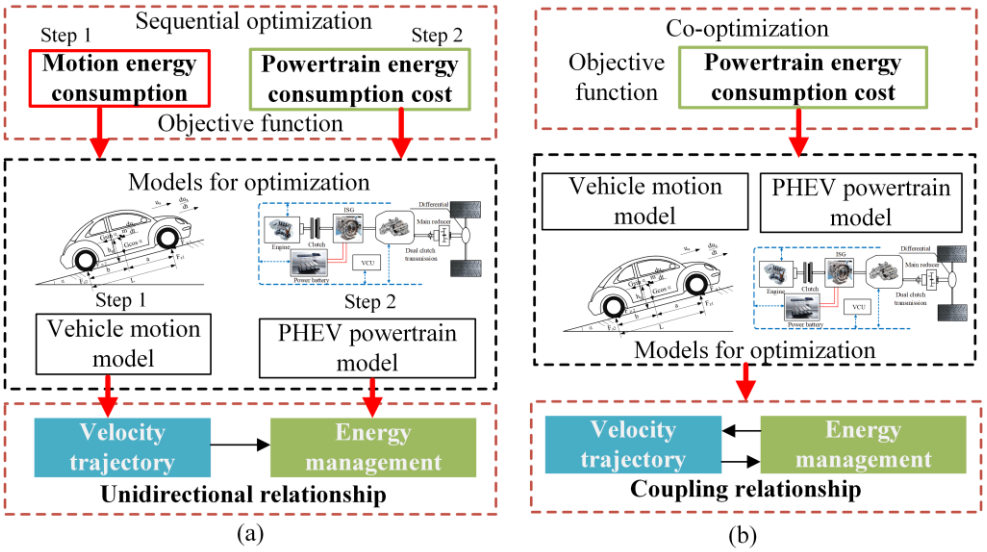

Fig. 1. The working principle of two optimal eco-driving control schemes. (a) sequential optimization, (b) co-optimization.

Motivated by the state-of-the-art discussion, this paper proposes an efficient optimal eco-driving approach for PHEVs based on a hierarchical data-driven framework, so as to overcome the incomplete decoupling in sequential optimization and mitigating the intensive calculation existing in co-optimization methods. The proposed framework

can be divided into two layers. In the upper layer, the velocity trajectory is optimized macroscopically. The energy consumption cost of the studied powertrain, i.e., the sum of fuel cost and electricity cost, is chosen as the optimization target. Then, an optimal energy consumption cost model and an optimal battery current model are constructed offline through two neural networks (NNs). Next, the NN based DP algorithm, incorporating the data-driven models and Bellman's optimality principle, is proposed to plan the driving speed. By this manner, the interaction between velocity and energy allocation is efficiently integrated in velocity optimization. In the lower layer, an optimal EMS is applied to find the control policy of the powertrain. Numerical simulations are conducted, and the results highlight that the proposed control strategy can properly planning the vehicle velocities, and simultaneously promote the energy management with preferable fuel economy. In addition, the simulation results reveal that the proposed method leads to high computational efficiency with only slight sacrifice on fuel economy, compared with the optimum benchmark.

The main contributions of this paper can be attributed to the following three aspects: 1) a data-driven based eco-driving control method for PHEV with real-time application capacity is systematically addressed to properly plan the speed and remarkably reduce the energy consumption; 2) the optimal energy consumption cost model and optimal battery current model for PHEV are constructed by two NNs based on the results obtained through DP; 3) the NN based DP is proposed, with two NNs considered as the critic model and the system model, to contribute to performance improvement in terms of fuel economy and calculation efficiency.

The remainder of this paper is structured as follows: Section II presents the mathematical modeling of the PHEV, and formulates the optimal control problem for eco-driving. Section III illustrates the construction of data-driven models and the data-driven optimal eco-driving approach. Section IV provides the detailed simulation analysis based on the proposed method. Finally, the main conclusions and future work are described in Section V.

II. MODELING AND PROBLEM DISCUSSION

To design the eco-driving controller for speed planning and energy management, the vehicle needs to be modeled, and the input and output of the controller should be defined.

A. Vehicle Model

The main target of eco-driving is to optimize the velocity profile. In this paper, the motion vehicle is supposed

to be limited by only longitudinal dynamics, and the impact of lateral dynamics is not taken into account. The required driving force can be expressed as:

$$F_v = \frac{1}{3600\eta_t}\left(Mgf\cos(\alpha) + \frac{\rho_{air} C_D A v^2}{2} + Mg\sin(\alpha) + \delta M \frac{dv}{dt} \right) \quad (1)$$

where M is the vehicle mass, f means the rolling resistance coefficient, g is the acceleration of gravity, α expresses the road grade, C_D denotes the air drag coefficient, A indicates the frontal area of the vehicle, ρ_{air} is the air density, v is the vehicle speed, δ is the correction coefficient of rotating mass, and η_t is the transmission system efficiency.

B. Powertrain System Model

The powertrain of the studied PHEV is with a parallel configuration, of which the structure is shown in Fig. 2. As can be found, the vehicle can be propelled individually by either the engine or the integrated starter generator (ISG), and the dual clutch transmission (DCT) is coupled with the main reducer and the motor axle to adjust their torque and speed ratios. To conduct high-quality speed planning, the powertrain efficiency of powertrain needs to be analyzed in detail.

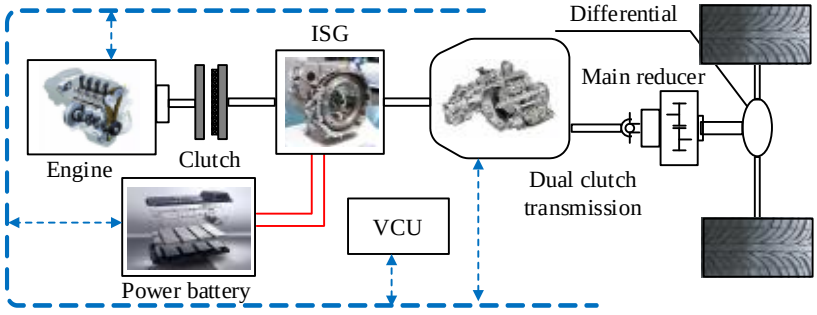

Fig. 2. Powertrain system of the PHEV.

The modeling of the studied PHEV mainly includes three parts: engine, ISG motor and power battery, and additionally the accessory power is neglected for simplification in this research. Moreover, the powertrain dynamics are usually neglected to simplify the design of eco-driving and energy management algorithms. The fuel consumption rate $\dot{m}_{fuel}$ (unit: g/kwh) is calculated by interpolating torque T_e and speed n_e, as:

$$\dot{m}_{fuel} = f_e(T_e, n_e) \quad (1)$$

where f_e denotes the nonlinear map acquired by the calibration experiment. Thus, the total fuel consumption

Q_{fuel} (unit: kg) can be formulated as:

$$Q_{fuel} = \int \frac{\dot{m}_{fuel} \cdot T_e \cdot n_e}{3.6 \times 10^6 \times 9500 \rho} dt \quad (1)$$

where ρ is the density of gasoline. Similarly, the efficiency model of ISG is acquired by the experimental data, and an interpolation model is constructed to describe the relationship among efficiency η_m, motor torque T_m and motor speed n_m, as:

$$\eta_m = f_m(T_m, n_m) \quad (1)$$

where f_m denotes the efficiency map of ISG. The battery power P_b can be formulated as:

$$P_b = \frac{T_m \cdot n_m}{9550 \eta_m} \quad (1)$$

An open circuit voltage source (OCV)- resistance model is adopted to characterize the battery's electrical performance. Based on the Kichoff's law, the battery current can be calculated, as:

$$I_b = \frac{E - \sqrt{E^2 - 4RP_b}}{2R} \quad (1)$$

$$SOC(t) = SOC_0 - \frac{\int_0^t I_b(t) dt}{Q_b} \quad (2)$$

where SOC_0 is the initial SOC, Q_b is the battery capacity, I_b is the battery current, E and R represent the open circuit voltage and the battery internal resistance, which can be acquired by interpolation. The electricity consumption Q_{ele} can be accumulated, as:

$$Q_{ele} = \int \frac{I_b \cdot E}{3.600 \times 10^6} dt \quad (3)$$

C. Eco-Driving Control Problem Formulation

In this study, the target of eco-driving control for PHEV is to minimize the cost of fuel and electricity consumption while properly planning the vehicle velocity for the designated driving missions. It is noteworthy that in this research, the eco-driving control is optimized in spatial domain, since the speed limit information is typically provided by intelligent traffic system (ITS) according to the current driving position. For actual applications, the

speed constraints can be constructed in terms of legal limit, road grade and traffic lights [33, 34]. For the studied PHEV, the total energy consumption cost of powertrain is defined as the objective function for eco-driving control. The control variables and state variables should include the characteristic parameters of vehicle motion and powertrain system. On this account, the control variables u consist of longitude acceleration a, ICE torque T_e, and DCT gear ratio i_{DCT}; and the state variables x include velocity, travel time as well as SOC. Thus, the optimal control problem of eco-driving can be formulated as:

$$J = \int_0^{s_f} \frac{dcost_{energy}(u,x)}{v(s)} ds \tag{3}$$

$$cost_{energy} = P_f \cdot Q_{feul} + P_e \cdot Q_{ele} \tag{3}$$

$$u = [a, T_e, i_{DCT}]^T \tag{3}$$

$$x = [v, t, SOC]^T \tag{3}$$

$$\frac{d}{ds}\begin{pmatrix} v \\ t \\ SOC \end{pmatrix} = \begin{pmatrix} \dfrac{a(k)\cdot t(k)}{2\cdot ds} \\ \dfrac{2\cdot ds}{v(k)+v(\mathrm{k}+1)} \\ -\dfrac{I_{\mathrm{b}}(t)dt}{Q_{\mathrm{b}}} \end{pmatrix} \tag{3}$$

where J denotes the objective function, $cost_{energy}$ represents the powertrain energy consumption cost, s_f indicates the total driving mileage, s means the driving distance, P_f and P_e denote the price of fuel and electricity. In addition, the constraints in terms of motion dynamics and powertrain limits should be imposed, as:

$$\begin{cases} SOC_{min} \le SOC \le SOC_{max} \\ n_{e\_min} \le n_e \le n_{e\_max} \\ T_{e\_min}(n_e) \le T_e \le T_{e\_max}(n_e) \\ n_{m\_min} \le n_m(k) \le n_{m\_max} \\ T_{m\_min}(n_m(k)) \le T_m(k) \le T_{m\_max}(n_m(k)) \\ v_{\min}(k) \le v(k) \le v_{\max}(k) \\ a_{\min}(k) \le a(k) \le a_{\max}(k) \end{cases} \tag{3}$$

Distinctly, it is difficult to directly solve the optimal control problem, since the massive control and state variables

can lead to curse of dimensionality. In addition, conventional sequential optimization methods failed to account for the relationship between velocity and powertrain characteristics. To tackle it, a computationally efficient control framework based on data-driven models is proposed to obtain high-performance eco-driving control of the PHEV.

III. DATA-DRIVEN ECO-DRIVING CONTROL

Based on the above analysis, direct solving of optimal eco-driving control is difficult to achieve. To solve this difficulty, a hierarchy control framework is derived for eco-driving control. To fully consider the relationship between velocity and powertrain characteristics in a hierarchical framework, a critical task is to construct a high-efficiency but accurate objective function to model the powertrain energy consumption during velocity optimization. To this end, two NN models, including one critic model and one system model, are established for modeling optimal energy consumption cost and optimal current; and a NN based DP algorithm is employed for velocity profile optimization. The structure of the proposed approach is shown in Fig. 3. In the offline modules, DP is exploited to prepare the optimal solution dataset for training. The online modules are divided into two parts: 1) date-driven velocity optimization, and 2) energy management optimization.

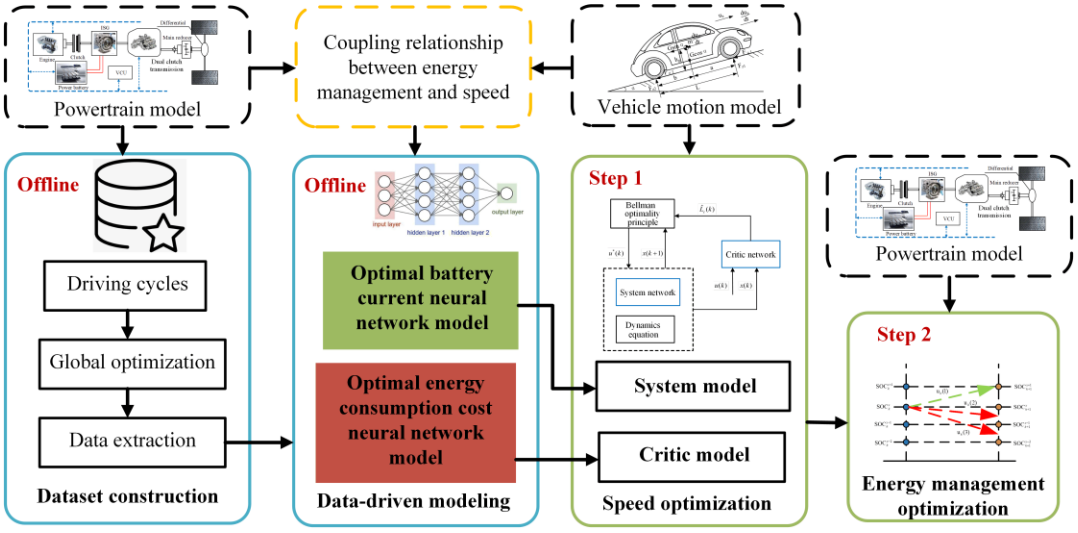

Fig. 3. The framework of data-driven based eco-driving control.

A. *Dataset Construction*

The dataset construction is divided into two steps: 1) the energy management is optimized by DP based on a comprehensive driving cycle, which involves different driving conditions; and 2) the result of global optimization is translated to optimal energy consumption cost and optimal current, then the dataset is extracted for model training.

Step 1: A comprehensive driving cycle, constituted by real-time driving scenarios, is shown in Fig. 4 (a) and

designed to contain different driving states of the vehicle. The optimal energy management is solved by DP with the objective function of cost minimization of energy consumption, as shown in (10). Our previous research reveals that the key variants impacting fuel economy of PHEVs include velocity, acceleration, driving distance and SOC [35]. While, the influence of driving distance and SOC can be illustrated by an equivalent distance factor L_{equ}, as:

$$L_{equ} = \frac{SOC_{rem} / SOC_{all}}{L_{rem} / L_{\max}} \tag{4}$$

where SOC_{rem} and SOC_{all} denote the remaining SOC and the maximum SOC when the battery is fully charged; L_{rem} and $L_{\max}$ denote the remaining driving distance and all-electric range. When L_{equ} is greater than or equals to 1, one inference can be made that electricity is enough to sustain the remain driving range. Hence, the upper limit is set as 1, and thus the range of L_{equ} is within [0, 1]; while $L_{\text{equ}} < 1$ means that the energy left in the battery cannot sustain the remaining trip, and the ICE needs to be engaged in driving the vehicle to destination. Thus, velocity, acceleration and equivalent distance factor are defined as the driving state of PHEV. The matrix of equivalent distance factor for the preferred driving cycle is calculated according to (15) and shown in Fig. 4 (b). The warm color indicates that ICE needs to participate in driving the vehicle. In contrast, the green area means that the electric energy is sufficient for the remaining trip.

Step 2: The DP algorithm is leveraged to obtain the optimal controlling sequence. However, the accumulated optimal cost-to-go matrix generated conversely and the optimal control decision matrix are critical in this study. The optimal energy consumption cost of each step is obtained by the difference calculation of the accumulated cost matrix, and partial optimal energy consumption matrix is presented in Fig. 4 (c). As can be seen, a remarkable increase trend is preferred with the decline of SOC at each step, and is in line with the variation of equivalent distance factor shown in Fig. 4 (b). The reason is that the ICE has to contribute more energy to vehicle propulsion. While, with the same SOC, the energy consumption cost difference between different steps is incurred due to the influence of velocity and acceleration.

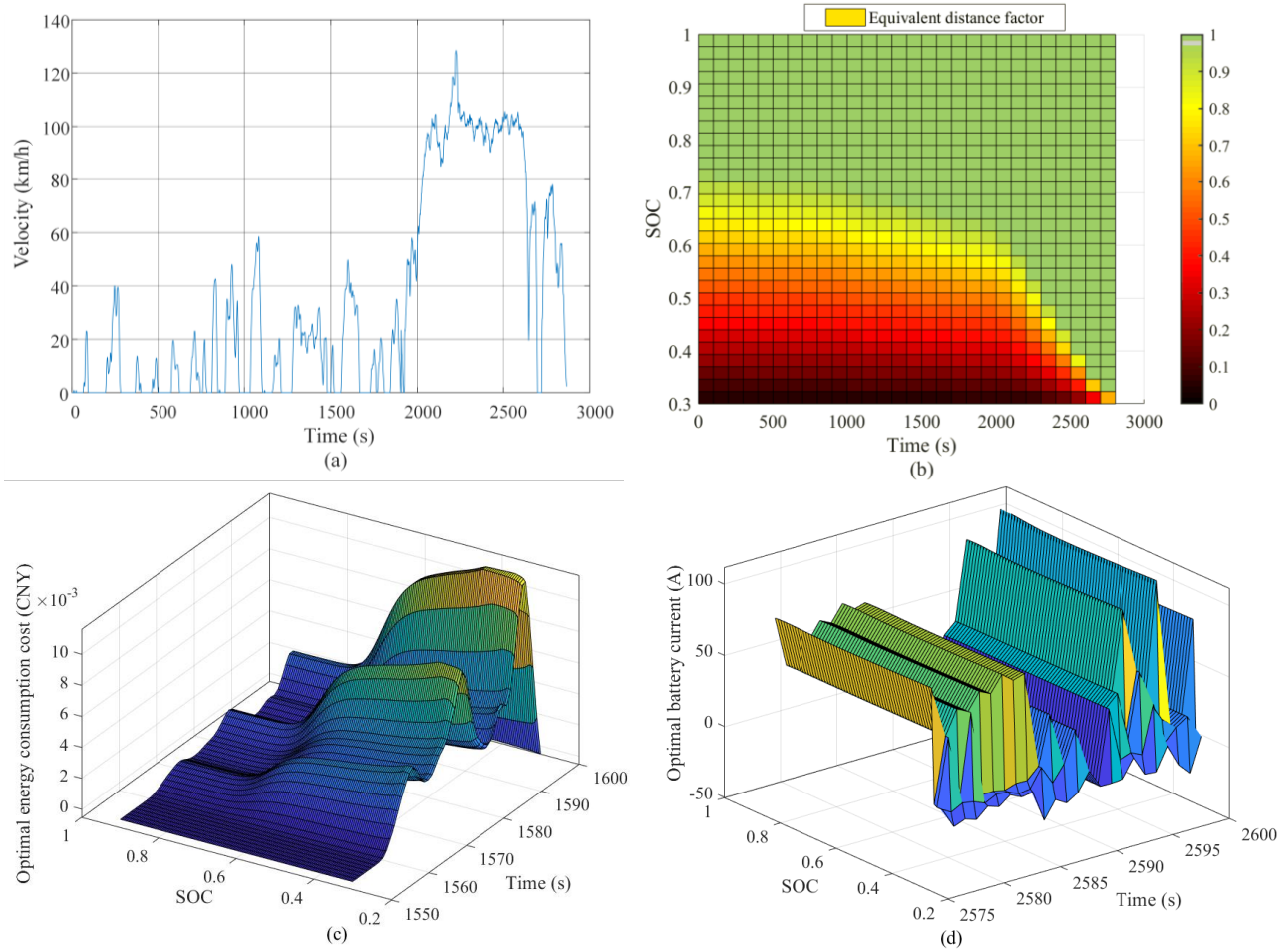

Fig. 4. Data sets for modeling. (a) comprehensive driving cycle, (b) equivalent distance factor matrix, (c) partial optimal energy consumptions cost matrix, (d) partial optimal battery current matrix.

Similarly, the optimal battery current matrix is calculated by (5) and (6) according to the optimal control decision matrix, and partial values are plotted in Fig. 4 (d). It can be observed that the optimal current tends to be positive when the SOC is high. Instead, the optimal current gradually becomes negative when the SOC is close to the lower limit. In this case, the PHEV typically operates in the energy recovery mode or charging mode to avoid SOC from dropping below the threshold. Thus, it can be summarized that the optimal current can adjust the SOC trajectory according to the driving state. By this manner, the dataset for data-driven modeling can be prepared, including the optimal energy consumption cost matrix, optimal battery current matrix, and equivalent distance factor matrix.

B. Data-Driven Modeling

The target of data-driven modeling is to estimate the energy consumption and state transfer of PHEV by incorporating the characteristics of powertrain but without directly employing the detailed powertrain component

models. In this study, two data-driven models are constructed, including one optimal energy consumption model and one optimal current model. Since the back propagation NN (BPNN) shows satisfactory fitting performance in mapping nonlinear data, and can adaptively adjust the weights and thresholds during training [36], two BPNNs with three layers are applied to construct the data-driven models. The gradient descent method is employed to search the optimal parameters of BPNNs in each iteration. For instance, the correction of weights is formulated by:

$$\Delta w_i = -\eta \frac{\partial R_e}{\partial w_i} \tag{5}$$

where η denotes the learning rate, R_e means the average root mean square error of training, and w_i is the weights for different neurons. The optimal energy consumption cost NN is treated as the critic model to output the optimal powertrain energy consumption cost at different driving states. The structure of critic network is shown in Fig. 5, where $\mathbf{w}_{\text{in}}$ represents the weighting vector between input layer and hidden layer, and $\mathbf{w}_{\text{out}}$ is the weighting vector between hidden layer and output layer. As can be found, the input vector $\mathbf{x}$ consists of v, a and L_{equ}, and the output is the estimated powertrain energy consumption cost $\hat{cost}_{energy}$, as:

$$\hat{cost}_{energy} = f_{NNC}(v, a, L_{equ}) \tag{6}$$

where f_{NNC} denotes the nonlinear map function describing the relationship between driving state and optimal energy consumption. The optimal current NN can be considered as a system model to output the optimal current according to the driving state. The optimal current will be applied for state transfer of SOC. Similarly, the input vector is the same as that of the critic model, which reflects the driving state of PHEVs. The output is the estimated optimal battery current $\hat{I}_b$, as:

$$\hat{I}_b = f_{NNS}(v, a, L_{equ}) \tag{7}$$

where f_{NNS} represents the nonlinear map function describing the relationship between driving state and optimal battery current. As presented before, the optimal energy consumptions cost matrix and the optimal battery current matrix are chosen to train the critic model and system model. The number of neurons, learning rates and the maximum iterations number are determined according to our experience and optimization iteration. Finally, the number of neurons is respectively set to 20 and 15 for the optimal energy consumption model and optimal current

model after iteration and optimization; the learning rate and maximum iterations number are defined as 0.05 and 300 for both NNs. In the next step, the optimal eco-driving control will be formulated and solved.

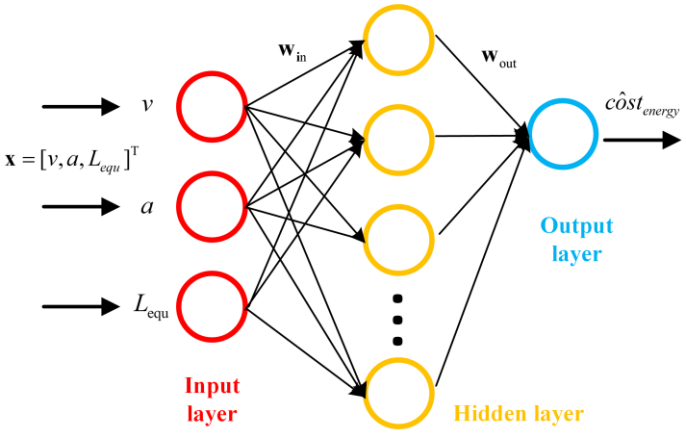

Fig. 5. Structure of optimal energy consumption cost network.

C. Data-Driven Velocity Optimization

As discussed before, the optimal eco-driving control is a nonlinear optimal control problem, and the velocity control module seeks optimal decisions that minimize the energy consumption of powertrain. Based on the Bellman's principle, DP can transfer complicated nonlinear optimal control problems into numerous sub-problems and raise global optimal solutions. However, standard DP is difficult to directly solve the optimal velocity for powertrain in a hierarchy framework, since the explicit powertrain models are difficult to be involved in velocity optimization. To tackle it, a NN based DP algorithm is proposed to find the optimal driving speed profiles for eco-driving.

The main purpose of NN based DP is to replace the cost function and state transfer function with two NNs which are trained offline according to the characteristics data of powertrain. It is essentially a heuristic method, and looks similar to adaptive dynamic programming (ADP) [37]. To improve the computational efficiency, most ADP methods typically leverage the NN based action model and critic model to avoid directly solving the Bellman optimality equation and find approximate optimal control decisions [38]. As shown in Fig. 6, the optimal energy consumption cost NN is defined as the critic model to estimate the approximate optimal powertrain energy consumption according to the state vector and control vector; and the backward recursive algorithm is employed to solve optimal control decisions, so as to mitigate the mapping error of action model by conventional ADP methods [39]. Nonetheless, the optimal current NN is chosen as the system model to estimate the optimal current policy based on different driving states, thus attaining SOC planning. By this way, the implicit powertrain models are

integrated in velocity optimization as a model-free manner, contributing to computation burden reduction.

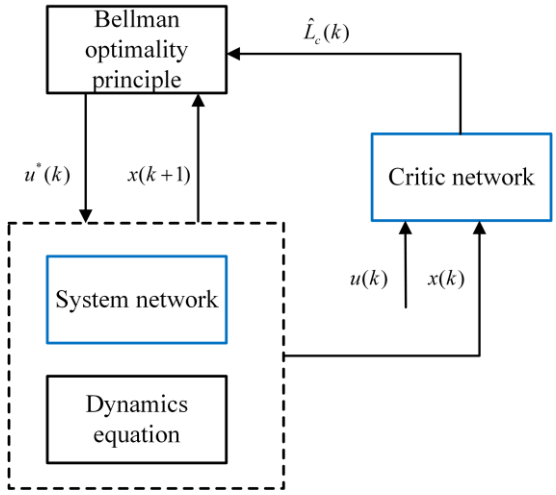

Fig. 6. Structure of NN based DP.

The objective function of data-driven velocity optimization in discrete form can be reformulated as:

$$J = \sum_{k=0}^{N-1} L(x_k, u_k) + L(x_N) \tag{8}$$

where $L(x_k, u_k)$ is the cost of each step. To further improve the computational efficiency, the travel time is eliminated from the state variable with the help of a penalty factor λ. Now, the cost function at each step can be expressed as:

$$L(x_k, u_k) = L_c(x_k, u_k) + L_t(x_k, u_k) \tag{9}$$

$$L_c(k) = \frac{f_{\mathrm{NNC}}(x_k, u_k) \cdot ds}{v(k)} \tag{10}$$

$$L_t(k) = \lambda \frac{ds}{v(k)} \tag{11}$$

where L_c represents the energy consumption cost of each stage, and L_t denotes the time cost of each stage. The designated arrival time can be guaranteed via adjusting the weight factor [32]. Thus, the objective function can be reformulated, as:

$$J = \sum_{k=0}^{N-1} \frac{f_{\mathrm{NNC}}(x_k, u_k) + \lambda}{v(k)} + L(x_N) \tag{12}$$

where $L(x_N)$ is the terminal cost to fulfill the driving mission, and can be determined according to the terminal constraints of velocity and travel duration. Based on the Bellman principle, the optimal control sequence u_k^* can

be solved by:

$$u_k^* = \arg\min\left\{L(x_k, u_k) + J^*(x_{k+1})\right\} \tag{13}$$

where $J^*(x_{k+1})$ represents the optimal accumulated cost in next step. Apparently, the powertrain characteristics are integrated into the objective function with the help of the critic model. Hence, the data-driven critic model can approximate the powertrain energy consumption, and eliminate the complicated powertrain models and control decisions. Finally, the control and state variables of data-driven velocity optimization can be summarized as:

$$u = a(s) \tag{14}$$

$$x = \begin{bmatrix} v & SOC \end{bmatrix}^T \tag{15}$$

$$v(k+1) = v(k) + a(k) \cdot t(k) \tag{16}$$

$$SOC(k+1) = SOC(k) + \frac{f_{NNS}(x_k, u_k)}{Q_b} \tag{17}$$

Note that (28) is deduced from (6) and (18). The velocity and SOC can illustrate the state variation of system in terms of vehicle motion and powertrain system. Similarly, the dynamics of SOC can also be considered according to (28) and the data-driven system model. It should be mentioned that the above calculations are realized by the data-driven models, rather than by the explicit powertrain model and the complicated powertrain control decision policy. By this manner, the simplification of optimal control solving is reached. In addition, the following constraints, including terminal constraints, still need to be imposed, as:

$$\begin{cases} v_{\min}(s) \le v(s) \le v_{\max}(s) \\ a_{\min} \le a(s) < a_{\max} \\ t(s_f) \le t_f \\ v(0) = v_0, v(s_f) = v_f \\ SOC(0) = SOC_0 \\ SOC_{\min} \le SOC \le SOC_{\max} \end{cases} \tag{18}$$

Furthermore, the designated arrival time, determined by the demand of passengers, can balance the energy consumption and travel duration. In the following section, different preset desired duration can be employed for simulation validation. To solve the optimal control via NN based DP, the control and state variables are discretized in spatial domain. Since the discretization accuracy can generate significant influence on velocity optimization, the

discretization steps are determined through iterations, as shown in Table 1.

Table 1 Parameters discretization of NN based DP

Parameters	Discrete step	Unit
Distance	10	m
Acceleration	0.1	m/s^2
Velocity	0.1	m/s
SOC	0.01	-

D. Energy Management Optimization

The powertrain energy allocation is optimized according to the result of velocity optimization. Apparently, it is a standard optimal control problem which has been widely investigated in previous research [40]. Furthermore, since the driving speed profile is preplanned, and can be reckoned as the prior knowledge, the global optimization performance is guaranteed. The powertrain energy consumption cost is chosen as the objective, and the control variable vector u_{e} contains engine torque T_{e} and DCT gear ratio i_{DCT}. The optimal control problem is formulated, as:

$$J_{\mathrm{e}} = \int_0^{s_f} \frac{dcost_{energy}(u_{\mathrm{e}}, x_e)}{v(s)} ds \tag{19}$$

$$u_{\mathrm{e}} = [T_{\mathrm{e}}, i_{\mathrm{DCT}}]^{\mathrm{T}} \tag{20}$$

$$x_{\mathrm{e}} = SOC \tag{21}$$

Additionally, the constraints of powertrain system are imposed:

$$\begin{cases} SOC_{min} \le SOC(k) \le SOC_{max} \\ n_{e\_min} \le n_e(k) \le n_{e\_max} \\ T_{e\_min}(n_e(k)) \le T_e(k) \le T_{e\_max}(n_e(k)) \\ n_{m\_min} \le n_m(k) \le n_{m\_max} \\ T_{m\_min}(n_m(k)) \le T_m(k) \le T_{m\_max}(n_m(k)) \end{cases} \tag{22}$$

Note that the optimal control of energy management is addressed via the typical DP algorithm in spatial domain. Based on the Bellman's principle, DP can transform complicated nonlinear optimal control problem into numerous sub-problems and raise global optimal solutions. More details about DP for EMS optimization can be found in our previous research [35]. In the next step, simulation analysis and discussions are performed to evaluate the performance of the proposed optimization framework.

IV. SIMULATION ANALYSIS

In this study, the discussed three eco-driving control strategies, including 1) sequential optimization scheme (simplified as S-opt), 2) co-optimization scheme (called C-opt) and 3) data-driven optimal eco-driving (referred to as D-opt hereinafter), are implemented for controlling performance comparison. Two cases studies are conducted to examine the control capability of the proposed eco-driving approach. The vehicle's basic parameters, from a product PHEV developed by Changan Automobile Ltd., are shown in Table 2. Note that the price of fuel is set as CNY 7.8 per liter, and the price of electricity is set as CNY 0.52 per kWh. Note that in this research, we not consider much about characteristic variation of the powertrain under different temperatures. As the maximum battery power and the ICE fuel rate are calculated by interpolation in this study, the proposed method will be still feasible in vehicle velocity planning and energy economy planning when the related calibration data under different temperatures are prepared. In addition, it is necessary to mention that the proposed algorithm can also be suitable for multi-objective optimization, such as energy economy promotion, battery life extension and greenhouse gas emission reduction, when the mentioned targets are included in the cost function.

Table 2 The basic parameters of objective PHEV

Characteristic	Value
Mass (kg)	1350
Frontal area (m^2)	2.82
Air drag coefficient	0.3146
Tire rolling radius (m)	0.308
Rolling resistance coefficient	0.0135
ISG peak power (kw)	40
Engine peak power (kw)	80
Battery capacity (Ah)	40
DCT gear ratio	3.917/2.429/1.436/1.021/0.848/0.667

In addition, the speed limits are presumed to obtain in advance via ITS and emerging vehicle-to-everything (V2X) communications. The adopted S-opt and C-opt are detailed in [32], and here we only refer to them for simplicity. For C-opt, the powertrain energy consumption cost is set as the objective function, and the optimal control problem can be formulated as：

$$J_c = \int_0^{s_f} \frac{dcost_{energy}(u_c, x_c)}{v(s)} ds \tag{23}$$

$$u_c = [a, T_e, i_{DCT}]^T \tag{24}$$

$$x_{\mathrm{c}} = \left[v, t, SOC\right]^{T} \tag{25}$$

where J_{c} represents the objective function, u_{c} is the control vector, x_{c} is the state vector. While, for S-opt, the optimization settings of EMS optimization remain the same as that of the proposed D-opt, as shown in (30) to (33); and the motion energy consumption is defined as the objective function for velocity optimization, as:

$$J_{S1} = \int_{0}^{s_f} \left(F_v(u_{\mathrm{s}}, x_{\mathrm{s}}) \cdot v\right) ds \tag{26}$$

$$u_{\mathrm{s}} = a(s) \tag{27}$$

$$x_{\mathrm{s}} = \left[v, t\right]^{T} \tag{28}$$

For comparison, both S-opt and C-opt are solved by the DP algorithm. Apparently, compared with D-opt and S-opt, C-opt is exposed to huge computational burden due to the massive control and state variables.

A. Case Study for Basic Driving Cycle

To examine the essential characteristics of different methods, a basic driving mission is constructed and requires the vehicle to drive for 1 km within 70 s. The initial and terminate speed is set to zero, and a constant high-speed limit of 30 m/s is chosen during the trip. As the driving mileage of the constructed basic driving cycle is quite short for PHEVs, the initial SOC is set to 0.31, thereby enabling the engine to participate in propelling the vehicle. The basic driving cycle can showcase the designed velocity profiles and the powertrain operating state by different control strategies, with a larger feasible range of speed planning. Additionally, such a simulation can also provide a reference for identifying the rules during velocity planning, since arbitrary driving cycles can be regarded as the combinations of numerous basic driving cycles [41].

The velocity optimization result is shown in Fig. 7 (a). Apparently, the velocity profile by D-opt highlights the similar trend as that by C-opt, and a moderate acceleration is observed at the beginning, followed by gradual deceleration. While, the speed profile obtained by D-opt exhibits higher acceleration and velocity between 100 m and 400 m. By contrast, the speed profile solved by S-opt exhibits a significantly different trend, compared with the other two methods. The speed shows drastic acceleration and deceleration in the beginning and ending of the trip, and the cruise driving occupies a large proportion of travel. It is interpretable that immoderate acceleration by S-opt is rendered to consume more energy when the knowledge of powertrain efficiency is inaccessible.

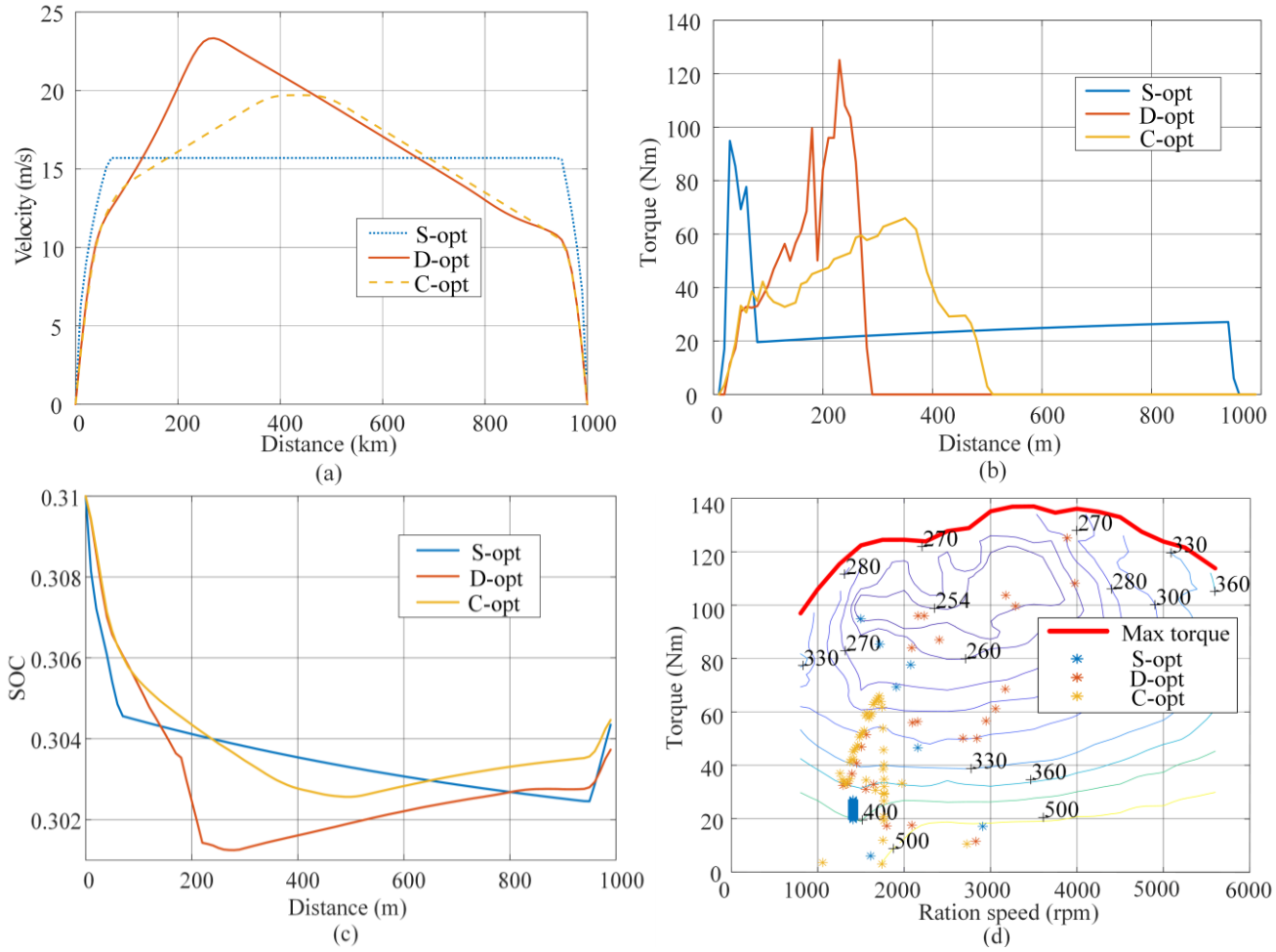

Fig. 7. Simulation results of basic driving cycle. (a) optimal velocity profiles, (b) engine torque, (c) SOC trajectories, (d) engine operating points.

The simulation results with respect to the powertrain are illustrated in Figs. 7 (b) to (d). As can be observed from Fig. 7 (b), the engine tends to operate during the acceleration through the control of C-opt and D-opt, and maintains off in the remaining range of coasting. By contrast, the engine by S-opt is on during most of the trip. On the other hand, as shown in Fig. 7 (c), an obvious increase in SOC emerges during coasting based on the D-opt and C-opt approach, indicating that electric energy recovery is conducted. While, the SOC trajectory generated by S-opt is decreasing during the cruise stage. As shown in Fig. 7 (d), most of the operating points by S-opt are located in low efficiency region between 20 Nm to 40 Nm due to the long duration of cruise. Apparently, the unreasonable velocity planning results in adverse impact on engine operation. While, the powertrain shows the similar operating state through the regulation of D-opt and C-opt. By contrast, S-opt enables the engine's engagement for longer driving time and lower operating efficiency. What is more, the inefficient engine operation state also deteriorates fuel economy when S-opt is applied. The fuel economy of three approaches is summarized in Table 3. As can be

seen, D-opt reduces the energy consumption cost by 22.1%, compared with S-opt. Additionally, D-opt leads to close energy consumption cost, compared with C-opt, which is treated as an optimal benchmark in this study. The fuel consumption by S-opt is distinctly higher than other two methods due to the improper engine engagement, leading to longer operating time and lower operating efficiency. To conclude, D-opt can generate similar control policy with C-opt in terms of velocity planning and powertrain control, and a remarkable improvement of fuel economy is achieved by D-opt, compared with conventional S-opt.

Table 3 Simulation results of fuel economy for basic driving cycle

Method	Energy consumption cost (CNY)	Reduction (%)	Fuel consumption cost (CNY)	Electricity consumption cost (CNY)
C-opt	0.238	24.0	0.202	0.036
D-opt	0.244	22.1	0.203	0.041
S-opt	0.313	-	0.276	0.037

B. Case Study for Complicated Driving Conditions

To further verify the performance of the proposed method, a more complicated driving scenario is constructed for simulation. First, a standard driving cycle UDDS is converted to imitate the varying speed limit in real traffic environment, and as introduced in [42], the speed profile is magnified and shrunk to generate upper and lower speed limits. We assume that all the potential influences of different driving conditions, including legal limit, traffic lights and inter-vehicle distance, are involved in the speed limit. Even when the driving conditions are subjected to variations due to external influences such as traffic and weather, the proposed algorithm can still be applied only if the speed limits involve all the changes. The desired arrival time is set to 1266 s, and the initial SOC is set to 0.4. The results of velocity profiles by the three methods are shown in Fig. 8 (a). During the segment of 2 km and 4 km, all the three approaches optimize the velocity profiles that are close to the lower limit, indicating that based on the pre-set arrival time, all three eco-driving control strategies can plan the driving speed reasonably, without unnecessary acceleration and energy consumption. One common knowledge is that in the premise of meeting the requirement of desired travel duration, higher driving speeds typically consume more energy for driving. The driving speed profiles obtained by D-opt and C-opt involve deceleration in coasting during the whole trip, especially for the segment of 9 km to 12 km. By contrast, the velocity planned by S-opt highlights more aggressive acceleration and deceleration. Furthermore, the driving speed solved by S-opt shows a larger proportion in cruise stage, compared with the other two methods.

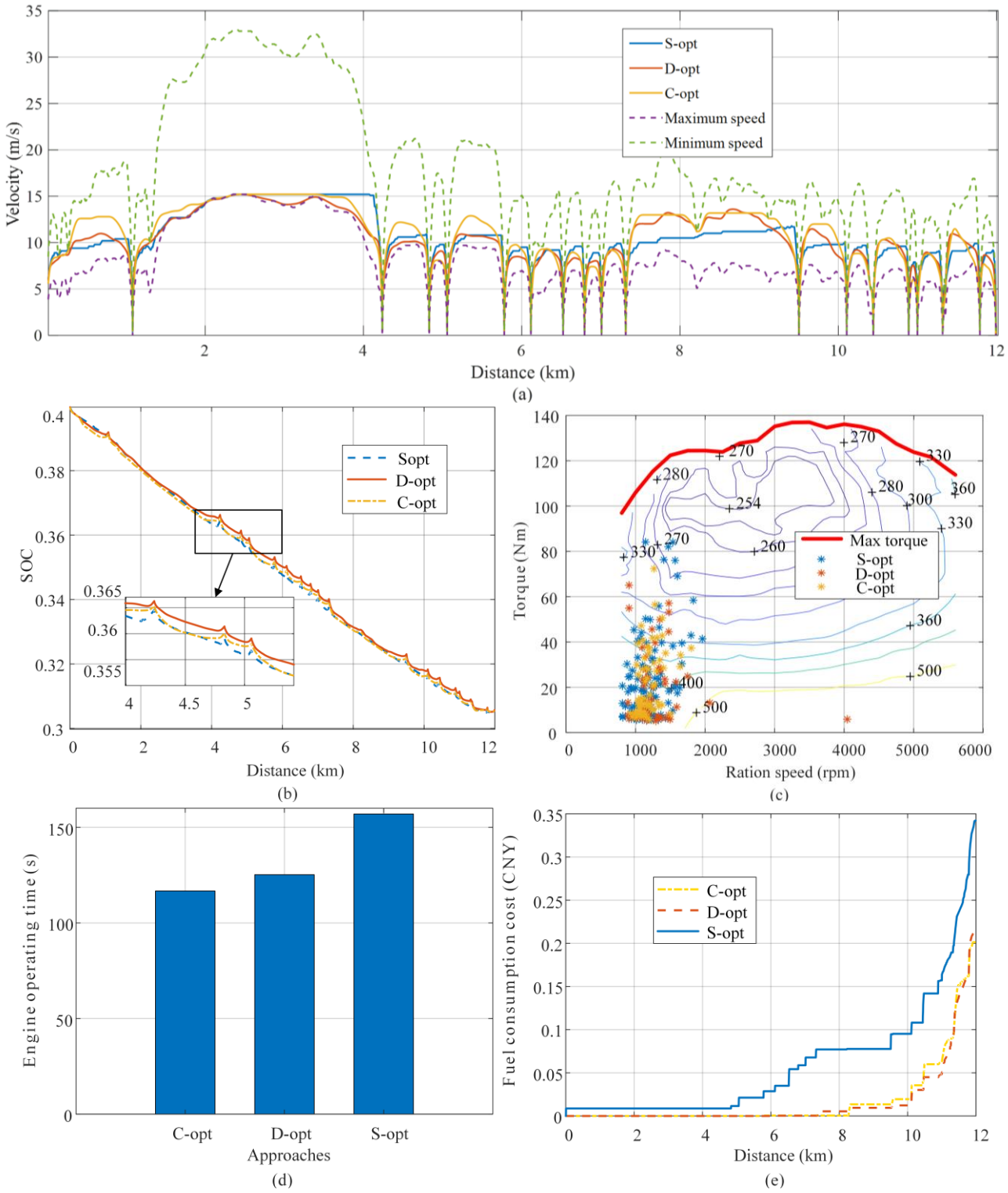

Fig. 8. Simulation results of complicated driving cycle. (a) velocity profiles for variable speed limit, (b) SOC trajectories, (c) engine operating points, (d) engine operating time, (e) fuel consumption cost.

The powertrain operation results are shown in Fig. 8 (b) and (c). As can be found in Fig. 8 (b), the SOC trajectories of three control strategies decrease almost linearly in spatial domain, and are in line with the global optimal SOC trajectory. Nonetheless, the distribution of engine operating points shows slight difference when

different control strategies are employed, as shown in Fig. 8 (c). It can be mainly attributed to two reasons: 1) narrow velocity planning range that makes the final solutions approximate due to the speed constraints, and 2) the same optimization algorithm for powertrain control that enables the engine with similar operating state. The simulation results are further discussed in Fig. 8 (d) and (e). As can be found in Fig. 8 (d), the engine operation duration (157 s) by S-opt is considerably longer than that by other two eco-driving approaches. Thus, it can be concluded that the increase of fuel consumption by S-opt is mainly attributed to the longer operating duration, since only slight difference of engine efficiency can be observed. Fig. 8 (e) compares the fuel consumption of different control strategies, and the fuel consumption cost by C-opt, D-opt and S-opt is CNY 0.2, 0.21 and 0.34, respectively. Apparently, S-opt generates extra fuel consumption during the segment of 5 km to 7 km, thanks to the improper velocity planning. Table 4 compares the simulation results, and we can summarize that the notable reduction in energy consumption cost (12.5%) is raised by D-opt, compared with conventional S-opt; and the fuel economy by D-opt is highly close to that by C-opt. However, S-opt shows the highest computational efficiency among the three methods, with the calculation time of 13.2 s. While, D-opt dramatically reduces the calculation time from 1487 s to 72.3 s, with a decrease of 95.1%, highlighting that D-opt can perform better in terms of computational efficiency and fuel economy. By contrast, S-opt obtains a minimum motion energy consumption of 0.653 kWh. The reason of causing the minimum motion energy consumption lies in that the motion energy consumption is defined as the objective function for velocity optimization, as analyzed in Section I and (37). Besides, the acceleration simulation results show that all three approaches have similar moderate average acceleration, which is located in the vicinity of 0.6 m/s^2. While, S-opt leads to a much higher average deceleration, compared with other two methods, thus imposing adverse effect on driving comfort. To sum up, compared with the optimum benchmark, D-opt can achieve the satisfied eco-driving result and the drastically improved calculation efficiency, reaching the anticipated control target.

Table 4 Simulation results of the complicated driving cycle

Method	Powertrain energy consumption cost (CNY)	Reduction (%)	Motion energy consumption (kWh)	Calculation time (s)	Average acceleration (m/s^2)	Average deceleration (m/s^2)
C-opt	0.83	13.5	0.754	1487.2	0.60	-0.53
D-opt	0.84	12.5	0.723	72.3	0.61	-0.48
S-opt	0.96	-	0.653	13.2	0.53	-1.22

To further validate the performance of D-opt, the simulations are conducted with different arrival time for more

in-depth discussion. The results are summarized in Table 5. It can be observed that D-opt improves the fuel economy significantly (averagely 13.5 %) under different arrival times. Additionally, the improvement shows an ascending tendency with the increase of desired arrival time. One main attribution can be speculated that longer desired arrival time can provide larger feasible region for velocity planning, and in this circumstance, D-opt can optimize the driving speed profile more reasonably. By contrast, shorter desired arrival time promotes the driving speed close to upper limit for meeting the demand of arrival time. To sum up, the proposed data-driven control scheme can lead to simultaneous speed planning and proper energy management with satisfactory performance and high efficiency.

Table 5 Simulation results for different desired arrival time

Desired arrival time (s)	D-opt			Reduction (%)	S-opt		
	Fuel consumption cost (CNY)	Electricity consumption cost (CNY)	Energy consumption cost (CNY)		Fuel consumption cost (CNY)	Electricity consumption cost (CNY)	Energy consumption cost (CNY)
1005	0.99	0.63	1.62	11.0	1.19	0.63	1.82
1126	0.49	0.63	1.12	13.9	0.67	0.63	1.30
1266	0.21	0.63	0.84	12.5	0.34	0.62	0.96
1405	0.05	0.60	0.65	16.7	0.16	0.62	0.78

V. CONCLUSIONS

This paper investigates a data-driven optimal eco-driving control strategy for PHEV with preferable performance and computational efficiency in terms of speed planning and energy management. The proposed algorithm can efficiently optimize the driving speed profile by incorporating the vehicle motion and powertrain system characteristics with the help of the built data-driven critic model and action model. A high-efficiency control framework is constructed, and two high-fidelity NN based data-driven algorithms are introduced as critic and system models for velocity optimization, mitigating the requirement of explicit complicated powertrain model. Then, the optimal eco-driving control problem is efficiently solved by NN based DP in spatial domain. The simulation results validate that the proposed approach can generate similar velocity profiles with the co-optimization scheme, and yet remarkably reduce the computational load by 95.1%. In addition, the energy consumption cost merely increases by 1.8%, compared with that by the co-optimization algorithm. As an extension, the proposed method can be applied to connected and automated vehicles with different powertrain systems, and can certainly contribute to energy-saving and control efficiency improvement.

The future research will be focused on further investigating eco-driving control strategies considering different

driving conditions and adaptively generating speed limits according to different potential disturbances, such as traffic lights and leading vehicles. To further make it close to actual applications, Pareto efficiency analysis will be leveraged for multi-objective optimization during eco-driving, so as to achieve a reasonable tradeoff between fuel economy, battery aging and driving comfort. Moreover, incorporating the influence of environment temperature into the modeling of powertrain system is another research direction in the future. Furthermore, advanced machine learning technologies, such as deep reinforcement learning, will be explored in eco-driving control to design more intelligent control schemes.

ACKNOWLEDGMENTS

The work is funded by the National Natural Science Foundation of China (No. 52002046) in part, Chongqing Fundamental Research and Frontier Exploration Project (No. CSTC2019JCYJ-MSXMX0642) in part, Science and Technology Research Program of Chongqing Municipal Education Commission (No. KJQN201901539) in part, and the EU-funded Marie Skłodowska-Curie Individual Fellowships Project (No. 845102) in part. Any opinions expressed in this paper are solely those of the authors and do not represent those of the sponsors.

REFERENCES

[1] R. Finesso, E. Spessa, and M. Venditti, "Robust equivalent consumption-based controllers for a dual-mode diesel parallel HEV," *Energy Conversion and Management,* vol. 127, pp. 124-139, 2016.
[2] T. Liu, B. Wang, and C. Yang, "Online Markov Chain-based energy management for a hybrid tracked vehicle with speedy Q-learning," *Energy,* Article vol. 160, pp. 544-555, 2018.
[3] J. Li, Y. Liu, D. Qin, G. Li, and Z. Chen, "Research on Equivalent Factor Boundary of Equivalent Consumption Minimization Strategy for PHEVs," *IEEE Transactions on Vehicular Technology,* Article vol. 69, no. 6, pp. 6011-6024, 2020, Art no. 9064599.
[4] Y. Liu, J. Liu, Y. Zhang, Y. Wu, Z. Chen, and M. Ye, "Rule learning based energy management strategy of fuel cell hybrid vehicles considering multi-objective optimization," *Energy,* Article vol. 207, 2020, Art no. 118212.
[5] K. Song, X. Wang, F. Li, M. Sorrentino, and B. Zheng, "Pontryagin's minimum principle-based real-time energy management strategy for fuel cell hybrid electric vehicle considering both fuel economy and power source durability," *Energy,* Article vol. 205, 2020, Art no. 118064.
[6] C. Sun, J. Guanetti, F. Borrelli, and S. J. Moura, "Optimal Eco-Driving Control of Connected and Autonomous Vehicles Through Signalized Intersections," *IEEE Internet of Things Journal,* Article vol. 7, no. 5, pp. 3759-3773, 2020, Art no. 8964352.
[7] A. Vahidi and A. Sciarretta, "Energy saving potentials of connected and automated vehicles," *Transportation Research Part C: Emerging Technologies,* vol. 95, pp. 822-843, 2018.
[8] X. He and X. Wu, "Eco-driving advisory strategies for a platoon of mixed gasoline and electric vehicles in a connected vehicle system," *Transportation Research Part D: Transport and Environment,* vol. 63, pp. 907-922, 2018.
[9] X. Qi, P. Wang, G. Wu, K. Boriboonsomsin, and M. J. Barth, "Connected Cooperative Ecodriving System Considering Human Driver Error," *IEEE Transactions on Intelligent Transportation Systems,* vol. 19, no. 8, pp. 2721-2733, 2018.
[10] L. Xie, Y. Luo, D. Zhang, R. Chen, and K. Li, "Intelligent energy-saving control strategy for electric vehicle based on preceding vehicle movement," *Mechanical Systems and Signal Processing,* vol. 130, pp. 484-501, 2019.
[11] S. Xu, S. E. Li, H. Peng, B. Cheng, X. Zhang, and Z. Pan, "Fuel-saving cruising strategies for parallel HEVs," *IEEE Transactions on Vehicular Technology,* Article vol. 65, no. 6, pp. 4676-4686, 2016, Art no. 7296694.
[12] J. Lee, D. J. Nelson, and H. Lohse-Busch, "Vehicle inertia impact on fuel consumption of conventional and hybrid electric vehicles using acceleration and coast driving strategy," *SAE Technical Papers,* Conference Paper 2009.
[13] Z. Ye, K. Li, M. Stapelbroek, R. Savelsberg, M. Gunther, and S. Pischinger, "Variable Step-Size Discrete Dynamic Programming for Vehicle Speed Trajectory Optimization," *IEEE Transactions on Intelligent Transportation Systems,* Article vol. 20, no. 2, pp. 476-484, 2019, Art no. 8320319.
[14] S. Xu, S. E. Li, K. Deng, S. Li, and B. Cheng, "A Unified Pseudospectral Computational Framework for Optimal Control of Road Vehicles," *IEEE/ASME Transactions on Mechatronics,* Article vol. 20, no. 4, pp. 1499-1510, 2015, Art no. 6926797.
[15] D. Shen, D. Karbowski, and A. Rousseau, "Fuel-Optimal Periodic Control of Passenger Cars in Cruise Based on Pontryagin's Minimum

Principle," *IFAC-PapersOnLine,* Article vol. 51, no. 31, pp. 813-820, 2018.
[16] J. Han, A. Sciarretta, L. L. Ojeda, G. De Nunzio, and L. Thibault, "Safe-and eco-driving control for connected and automated electric vehicles using analytical state-constrained optimal solution," *IEEE Transactions on Intelligent Vehicles,* vol. 3, no. 2, pp. 163-172, 2018.
[17] J. Han, A. Vahidi, and A. Sciarretta, "Fundamentals of energy efficient driving for combustion engine and electric vehicles: An optimal control perspective," *Automatica,* Article vol. 103, pp. 558-572, 2019.
[18] A. S. M. Bakibillah, M. A. S. Kamal, C. P. Tan, T. Hayakawa, and J. I. Imura, "Event-Driven Stochastic Eco-Driving Strategy at Signalized Intersections from Self-Driving Data," *IEEE Transactions on Vehicular Technology,* Article vol. 68, no. 9, pp. 8557-8569, 2019, Art no. 8778707.
[19] Z. Wang, G. Wu, and M. J. Barth, "Cooperative Eco-Driving at Signalized Intersections in a Partially Connected and Automated Vehicle Environment," *IEEE Transactions on Intelligent Transportation Systems,* Article vol. 21, no. 5, pp. 2029-2038, 2020, Art no. 8704319.
[20] H. Dong, W. Zhuang, G. Yin, H. Chen, and Y. Wang, "Energy-optimal velocity planning for connected electric vehicles at signalized intersection with queue prediction," in *IEEE/ASME International Conference on Advanced Intelligent Mechatronics, AIM*, 2020, vol. 2020-July, pp. 238-243.
[21] F. Zhang, X. Hu, R. Langari, and D. Cao, "Energy management strategies of connected HEVs and PHEVs: Recent progress and outlook," *Progress in Energy and Combustion Science,* vol. 73, pp. 235-256, 2019.
[22] D. Maamria, K. Gillet, G. Colin, Y. Chamaillard, and C. Nouillant, "Computation of eco-driving cycles for Hybrid Electric Vehicles: Comparative analysis," *Control Engineering Practice,* Article vol. 71, pp. 44-52, 2018.
[23] G. P. Padilla, S. Weiland, and M. C. F. Donkers, "A Global Optimal Solution to the Eco-Driving Problem," *IEEE Control Systems Letters,* Article vol. 2, no. 4, pp. 599-604, 2018.
[24] S. E. Li, H. Peng, K. Li, and J. Wang, "Minimum fuel control strategy in automated car-following scenarios," *IEEE Transactions on Vehicular Technology,* Article vol. 61, no. 3, pp. 998-1007, 2012, Art no. 6126064.
[25] B. Chen, S. A. Evangelou, and R. Lot, "Series Hybrid Electric Vehicle Simultaneous Energy Management and Driving Speed Optimization," *IEEE/ASME Transactions on Mechatronics,* vol. 24, no. 6, pp. 2756-2767, 2020.
[26] J. Hu, Y. Shao, Z. Sun, M. Wang, J. Bared, and P. Huang, "Integrated optimal eco-driving on rolling terrain for hybrid electric vehicle with vehicle-infrastructure communication," *Transportation Research Part C: Emerging Technologies,* vol. 68, pp. 228-244, 2016.
[27] S. Xie, X. Hu, T. Liu, S. Qi, K. Lang, and H. Li, "Predictive vehicle-following power management for plug-in hybrid electric vehicles," *Energy,* vol. 166, pp. 701-714, 2019.
[28] S. Wang and X. Lin, "Eco-driving control of connected and automated hybrid vehicles in mixed driving scenarios," *Applied Energy,* Article vol. 271, 2020, Art no. 115233.
[29] S. Qiu, L. Qiu, L. Qian, and P. Pisu, "Hierarchical energy management control strategies for connected hybrid electric vehicles considering efficiencies feedback," *Simulation Modelling Practice and Theory,* Article vol. 90, pp. 1-15, 2019.
[30] G. Heppeler, M. Sonntag, and O. Sawodny, "Fuel efficiency analysis for simultaneous optimization of the velocity trajectory and the energy management in hybrid electric vehicles," in *IFAC Proceedings Volumes (IFAC-PapersOnline)*, 2014, vol. 19, pp. 6612-6617.
[31] F. Mensing, E. Bideaux, R. Trigui, J. Ribet, and B. Jeanneret, "Eco-driving: An economic or ecologic driving style?," *Transportation Research Part C: Emerging Technologies,* Article vol. 38, pp. 110-121, 2014.
[32] Y. Kim, M. Figueroa-Santos, N. Prakash, S. Baek, J. B. Siegel, and D. M. Rizzo, "Co-optimization of speed trajectory and power management for a fuel-cell/battery electric vehicle," *Applied Energy,* vol. 260, p. 114254, 2020.
[33] H. Abbas, Y. Kim, J. B. Siegel, and D. M. Rizzo, "Synthesis of Pontryagin's Maximum Principle Analysis for Speed Profile Optimization of All-Electrified Vehicles," *Journal of Dynamic Systems Measurement and Control,* vol. 141, no. 7, 2019.
[34] G. Heppeler, M. Sonntag, U. Wohlhaupter, and O. Sawodny, "Predictive planning of optimal velocity and state of charge trajectories for hybrid electric vehicles," *Control Engineering Practice,* Article vol. 61, pp. 229-243, 2017.
[35] Z. Lei, D. Qin, P. Zhao, J. Li, Y. Liu, and Z. Chen, "A real-time blended energy management strategy of plug-in hybrid electric vehicles considering driving conditions," *Journal of Cleaner Production,* Article vol. 252, 2020, Art no. 119735.
[36] G. Hwang *et al.*, "Prediction of Hybrid Electric Bus Speed Using Deep Learning Method," *SAE Technical Papers,* Conference Paper vol. 2020-April, no. April, 2020.
[37] F.-Y. Wang, H. Zhang, and D. Liu, "Adaptive dynamic programming: An introduction," *IEEE computational intelligence magazine,* vol. 4, no. 2, pp. 39-47, 2009.
[38] G. Li and D. Görges, "Ecological adaptive cruise control and energy management strategy for hybrid electric vehicles based on heuristic dynamic programming," *IEEE Transactions on Intelligent Transportation Systems,* vol. 20, no. 9, pp. 3526-3535, 2018.
[39] G. Li and D. Görges, "Ecological Adaptive Cruise Control for Vehicles With Step-Gear Transmission Based on Reinforcement Learning," *IEEE Transactions on Intelligent Transportation Systems,* 2019.
[40] Y. Wu, Y. Zhang, G. Li, J. Shen, Z. Chen, and Y. Liu, "A predictive energy management strategy for multi-mode plug-in hybrid electric vehicles based on multi neural networks," *Energy,* Article vol. 208, 2020, Art no. 118366.
[41] B. Chen, S. Evangelou, and R. Lot, "Hybrid Electric Vehicle Two-step Fuel Efficiency Optimization with Decoupled Energy Management and Speed Control," *IEEE Transactions on Vehicular Technology,* 2019.
[42] C. Zheng, G. Xu, K. Xu, Z. Pan, and Q. Liang, "An energy management approach of hybrid vehicles using traffic preview information for energy saving," *Energy Conversion and Management,* vol. 105, pp. 462-470, 2015.